Iranian Journal of Hydrogen & Fuel Cell 1(2021) 1-12

Iranian Journal of Hydrogen & Fuel Cell

IJHFC

Journal homepage://ijhfc.irost.ir

Quantitative study of water level control system in PEM fuel cell separator for conservation of reactant gases

S.M. Rahgoshay[1,a], M. Rahimi-Esbo[b], M. Khorshidian[c]

[a] Researcher, PhD, North Institute of Science & Technology, Malek Ashtar University of Technology, Iran.
[b] Assistant professor, North Institute of Science & Technology, Malek Ashtar University of Technology, Iran.
[c] Researcher, MSc, North Institute of Science & Technology, Malek Ashtar University of Technology, Iran.

Article Information

Article History:

Received:
12 Oct 2020
Received in revised form:
31 Jan 2021
Accepted:
02 Feb 2021

Keywords

Fuel cell
Venturi
Water level control system
Quantitative study
Pressure drop

Abstract

One of the products of the interaction between hydrogen and oxygen in a fuel cell is water. The presence of this product can reduce the efficiency of the fuel cell and causes problems in its operation. The present study aims to introduce a water level control system that can prevent the loss of reactant gases, such as hydrogen and oxygen, by improving the process of separation of water from these gases. Thus, unused gases are returned to the fuel cell, and as a result, the costs of using the reactant gases for producing electric power will be reduced. Although the process of a control system has been described qualitatively in previous studies, this paper is intended to quantify this procedure with respect to fuel cell specifications and construction limitations. This system consists of mechanical (venturi) and control units and is designed based on different reactant gases such as air and oxygen. The fuel cell pressure drop and maximum wasted volume of gases when using this system are less than 0.001 bar and 0.5% in each cycle, respectively. This system is simulated based on different fuel cell operating pressures.

*Corresponding Author: rahgoshay@mut.ac.ir
majid.rahgoshay@gmail.com

doi: 10.22104/ijhfc.2021.4457.1211

Nomenclature

A	Cross section of venturi, mm^2	P_1	Position of pressure sensor,mm
C	Safety factor	P_2	Position of pressure sensor,mm
D_1	Diameter of connector,mm	P_s	Static pressure,Pa or bar
D_2	Diameter of venturi,mm	P_t	Total pressure,Pa or bar
D_3	Diameter of throat, mm	Q	Volume flow rate
F	Faraday's constant, C/mol	R_1	Radius,mm
H_1	Connectors height, mm	S	Stoichiometry
H_2	Height of convergence part of connector , mm	$T_{operating}$	Operating temperature, $^{\circ}K$
		t	Time,s
I	Electrical current,A	V_{net}	Volume of control system,mm^3
L_1	Input Length of venturi,mm		
L_2	Length of throat, mm	**Greek symbol**	
L_3	Output Length of venturi,mm		
$\dot{m}$	Mass flow rate ,Kg/s	$\bar{V}$	Velocity,mm/s
n_{cell}	Number of fuel cell	φ_i	Relative humidly

1.Introduction

The energy crisis, fossil fuel constraints, and air pollution caused by charcoal fuel have increased the focus on using new energy sources. Power generation by the fuel cell is one of these new sources based on the use of hydrogen. The use of hydrogen as a source of energy production can reduce environmental pollutants and remove sulfur oxides produced by burning fossil fuels. A single fuel cell can generate about 1 volt. Therefore, to reach high operating voltage, a large number of fuel cells are connected to form a stack, which forms part of the fuel cell cascade. The process of producing energy in a fuel cell also produces water due to the reaction between oxygen and hydrogen. This excess water requires the use of a separator combined with a water level control system between two successive stacks in the fuel cell cascade to prevent flooding in different parts of the fuel cell and a reduction of its performance [1].

Schwinger et al. [2] are the first researchers to model polymer membrane fuel cells. In the initial model of the fuel cell they assumed that water exists only in gas form, and a two-phase flow was not considered. The transfer of water was considered for the first time in fuel cell modeling in 2000. After that, several two-phase flow models were used, including the multiphase model [3], the mixed model of the volume of fluid, the permeable network model, and the Lattice Boltzmann method [4]. These methods are used to simulate different parts of the fuel cell, including the reactant output section, the shape of the reactant channel [5], etc.

A lot of research has been done to find methods to separate or detect water produced from reactant gases at the fuel cell outlet, which has the least amount of reactant loss. Internal and external water separators are most commonly used in fuel cells. External water separators are located outside the main cascade of the fuel cell [6]. Bowl water separator, Self-controlling separator [7], and Membrane separator [8] are examples of this type. Charlat et al. [9] used centrifugal force to separate water from gas in a fuel cell. They used a two-pipe channel in which the inner tube wall and internal part of the outer tube were hydrophilic, and an impeller inside the inner tube creates vortices. The mixture produced by the impeller follows along an approximately helicoid path in the internal space, and the water initially present in the mixture is pressed against the internal walls of the inner tube by centrifugal force. At the end of the process, suction is applied to carry the water out of the second tube. In a fuel cell system, the water and inert gases will collect in the last stack, where the inert gas is simultaneously be added to the reactants gases. This diluting of the reactant gases will cause a voltage drop in the fuel cell. Bette et al. [10] use the voltage drop as a control signal to open the purge valve. The voltage tap is carried out between the gas outlet and the purge valve, especially on a bipolar plate, and it can provide a sensitive and precise control by means of a lower voltage tap in comparison with a higher one. By

preventing reduce of voltage in the purge cell, risk of corrosion will be maintained at a minimum level for the bipolar plate. Schaefer et al. [11] combined an anode bleed valve and an anode drain valve into a single valve to perform both the bleed and drain functions to reducing the complexity of the fuel cell system. They proposed this valve be located in the water separation device at the bottom of the holding tank. They added tube bundle flow restrictions for providing a cathode inlet gas to each stack. The fuel cell cascade includes two pipes. The first pipe provides cathode gas flow to the first stack of the fuel cell cascade, and the second pipe receives cathode exit gas from the first stack and fresh cathode gas, send a combination of these gases to second one.

In addition to the methods presented, an orifice plate and venturi meter is another method that uses the differential pressure of the fluid to detect or separate water in a fuel cell. An orifice plate and venturi meter is the most common flowmeter instrument for both single and two-phase fluid flow. The function of this equipment is based on the differential pressure measurement of the fluid. A lot of experimental research and theoretical studies have been done to achieving useful measurement models (correlations or equations) for these flow meters [12]. Steven [13] lists seven correlations, two wet gas venturi correlations and five older orifice plates, and compares their performance with new independent data from the NEL wet gas loop. Jain et al. [14] analyzed and optimized two types of three-dimensional venturi meters, circular and slit, based on various geometrical parameters. Meng et al. [15] introduced a new method for air–water two-phase flow measurement using a venturi meter combined with an Electrical Resistance Tomography (ERT) sensor. This method solves the difficulty of mass quality measurement in conventional differential pressure based flowmetry techniques. Huang et al. [16] combined an ECT system and a venturi meter for the measurement of the flow rate of gas–oil two-phase flow. Umayahara et al. [17] used changes in the fluid pressure in a fuel cell separator system to detect the flow type in the purge channel. The opening and closing time of the valve was completely dependent on the pressure of the fluid.

Alizadeh et al. [18] designed a cascade-type PEM fuel-cell stack to achieve a lower reactant gas purge and higher efficiency. They divided the stack into several small stages, so that the outlet gas of each stage re-entered the next stage after passing through the separators. In this design, a separator must be used for the output of each stage. It is importance to use a separator because it separates the produced water and the condensate water from the reactive gases. This will prevent water from entering, as an impurity, into the next stage. If the separator malfunctions, two things will happen:

1) The separator does not drain the water: Water enters the next stage, this process is important since it can cause a severe irreversible voltage drop in the MEA.

2) The separator drains too much reactant gas: The amount of purge gases increases and the efficiency decreases. There may also be safety hazards.

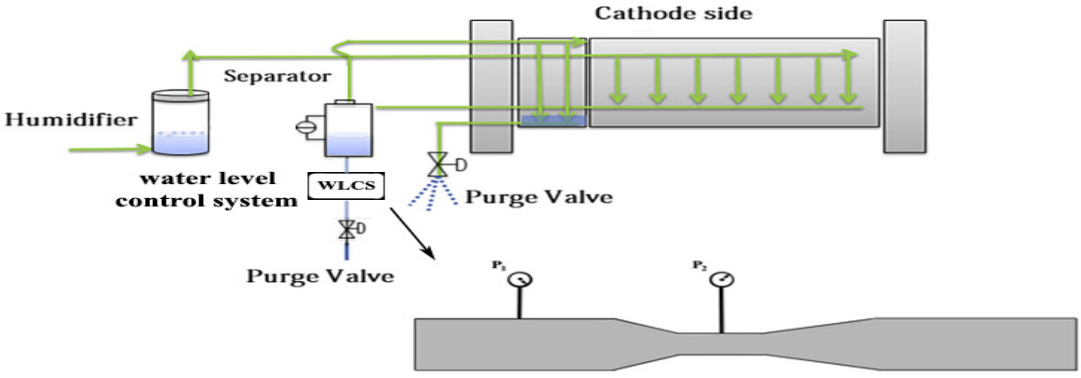

Fig. 1. Schematic illustration of the proposed water level control system.

This paper introduces an external water level control system (WCLS). Although the process of a control system has been qualitatively described by Dieter e al. [19], this paper intends to quantify this procedure with respect to fuel cell specifications and construction limitations. As shown in Figure 1, this system is used between the two stages of the stack to control the level of the water accumulated in the separator tank. It is consists of mechanical (venturi) and control units. First, the mechanical unit, which consists of a venturi and a differential pressure sensor, measures the variations of the pressure of the fluid passing through the venturi. Second, the control unit determines the type of fluid by analyzing the data received from the mechanical unit and then exports the next commands, such as opening or closing purge valve, to the other units. This system can be used instead of a conventional separator control system, such as a liquid level sensor in the separation tank. The construction cost of this new system not only is low, but it also has high sensitivity and precision in determining the type of fluid as well as being more durable than other control systems. This system was simulated based on the different operating pressures of a fuel cell.

Considering the water level control system is external, the working pressure is the only parameter that changes and influences it. In other words, changing the pressure of the fuel cell causes changes in both the differential pressure of the venturi and the criteria for determining the type of fluid. However, other factors, such as water produced and exit gases, that play a central role in determining different parameters of the control system are calculated based on fuel cell specification. As a result, the information required for a quantitative expression of the water level control system is divided into two general sections, theoretical calculation and simulations.

2.Theoretical calculation

In this section, the flow rate of the produced water and exit reactant gases are calculated based on the theoretical correlation of the fuel cell [20]. These parameters influence the determination of the dimensions of the venturi so that it can discharge enough water from the separator tank and minimize the loss of reactant gases. Assumptions used for determining the flow rate of the produced water and exit reactant gases are shown in Table 1.

Table 1: Initial Conditions of the Fuel Cell

S_{o_2}	2
$T_{operating}$	$330\,^{\circ}K$
n_{cell}	50
F	96485C/mol
ϕ_i	0.6

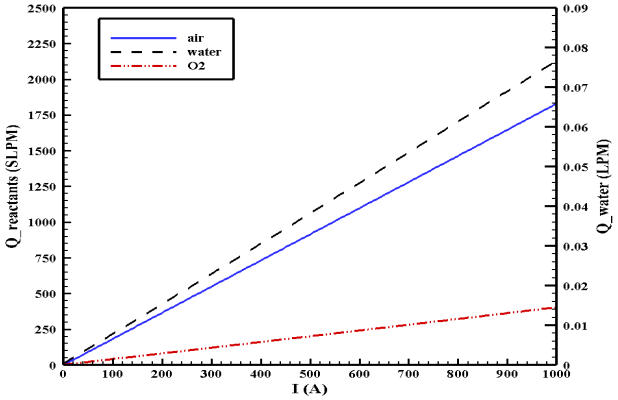

Fig.2. The flow rate of water and reactant gases in different electrical currents.

Figure 2 shows the flow rate of the produced liquid water and exit reactant gases for different electrical currents of the fuel cell. According to the high flow rate of exit gases, a large amount of reactor gases is needed to achieve a high electrical current.

3.Simulation

In this section, changes in the pressure of fluid flow through the venturi have been investigated based on different inlet gauge pressures of fluid to determine the types of flow and discharge flow rate of the fluid from the venturi.

3.1.Geometry

The venturi is named after the Italian scientist Batista Venturi. The main use of a venturi is to measure the discharged flow rate of fluid in pipes. It contains an input section (convergent), throat, and an output section (divergent). The velocity of fluid increases when it passes through the nozzle and reaches its maximum at the narrowest point, where the pressure will simultaneously be the lowest. Finally, the flow rate is calculated using the differential pressure difference. The convergence angle is 21 ± 1°, even though this angle is more suitable for liquids than gases. An angle between 7° and 15° was selected for the divergent section [21]. The geometry of this research has two parts. The first part, as shown in Figure 3- left side, is the connector of the venturi and the separator tank, which has a larger cross-section than the venturi. The second part of the geometry, as depicted in Figure 3-right, is a venturi, which has a longer inlet length in order to provide an appropriate space for the development of the inlet flow. Table 2 demonstrates the dimensions of different parts of the system and the position of P1 and P2, two points for measuring the differential pressure of the fluid. Divergence and convergence angles are considered 21° and 11°, respectively. It is worth noting that the minimum and maximum diameter of the venturi is based on experimental setup limitations.

Table 2. Geometric Dimensions of the Control System (mm)

D1	15.25	L1	30
D2	3.05	L2	10
D3	0.6-0.8	L3	30
H1	20	P1	21
H2	5	P2	39
R1	3.5		

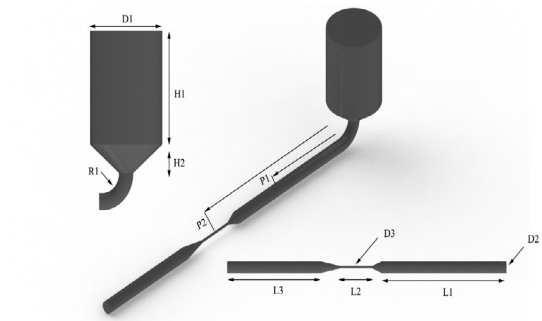

Fig.3. The geometry of the system.

3.2. Validation

Figure 4 shows the experimental data from the Mechanical Sciences Laboratory of Babol Noshirvani University of Technology used to validate the water simulation.

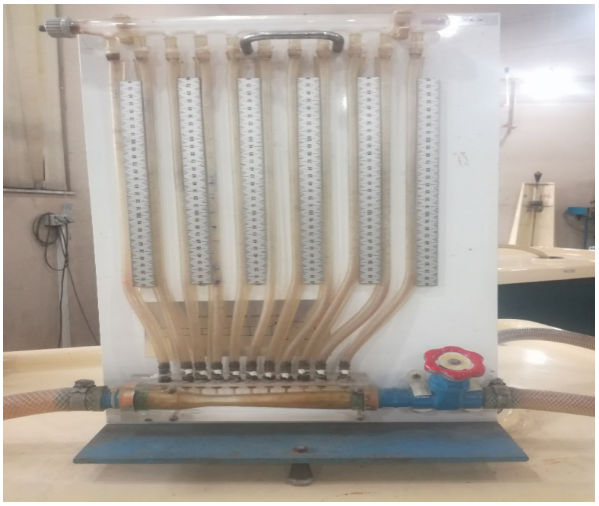

Fig.4. Image of the experimental setup.

As depicted in Figure 5, the change of fluid height from the simulation is close to the experimental data. Also, the data obtained by Shariatzadeh et al. is used as a reference for validating the reactant gases [22].

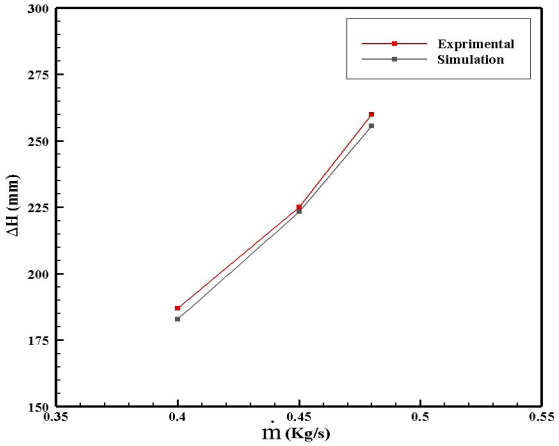

Fig.5. Validation of the working fluid water.

3.3.Simulation setup & independency of mesh

Several elements from 780000 to 1350000 were examined in order to achieve independency of the grid. The criterion used for grid independence is static pressure. Based on Figure 6, the static pressure at the upstream side of the convergent section experienced little change for more than 960000 elements. However, the throat was more sensitive than other parts of the venturi due to high changes in pressure and the occurrence of shock. As shown in Figure 6, the static pressure will have less than 50 Pa changes for the number of elements greater than 1150000. Therefore, 1150000 structured elements were selected for further simulations.

The boundary conditions of the geometry are as follows:

- Inlet and outlet are pressure based.
- No-slip condition is considered for the walls.

There are several turbulent flow patterns for simulating the problem. Initially, the operating fluids, including water, air, and oxygen, are simulated with the assumption of an incompressible flow at an inlet gauge pressure of 0.2 bar, the lowest pressure. Results indicate that the Mach number is less than 0.3 for the water and more than 0.3 for the air and oxygen. Therefore, in the simulation, water and reactant gases are considered incompressible and compressible, respectively. Moreover, the k-ε model was used as the turbulent model for simulating the turbulent flow.

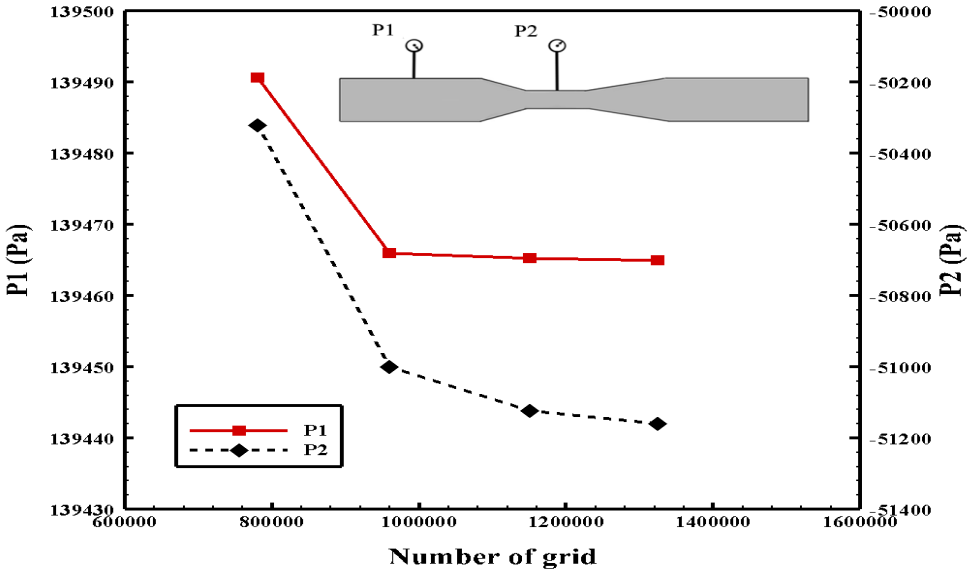

Fig.6. The grid independency for two points of the venturi.

4.Results and discussion

Three different fluids including oxygen, air and water are simulated for different pressure inlet with the range of 0.4 to 2 bar. At first, two venturi with different throat diameters of 0.6 and 0.8 mm are compared. At inlet gauge pressure of 1 bar, the discharge flow rate of the ventures are 0.208 and 0.424 LPM, respectively. According to Figure 2, the maximum discharged water for electrical current of 1000 A is 0.0767 LPM. Although both types can be used, fluid loss is lower in venturi with throat diameter of 0.6mm. Therefore, 0.6mm is selected for following simulation. Results of different variables such as pressure, discharged flow rate are described separately in following section:

4.1. Pressure of fluid

Liquid fluid, water, faces with higher pressure drop than gases, such as air and oxygen due to its incompressibility and high viscosity. As a result, at a certain inlet gauge pressure, the pressure of the water is less than the reactant, gases in the throat (Figure 7-A). On the other hand, as mentioned in the previous section, change of static pressure of the fluid, between throat and the upstream of the converging part, is the main factor for determining the type of fluid (Figure 7-B). Therefore, one of the two mentioned models can be used in order to detect the type of fluid, which is described in more details below:

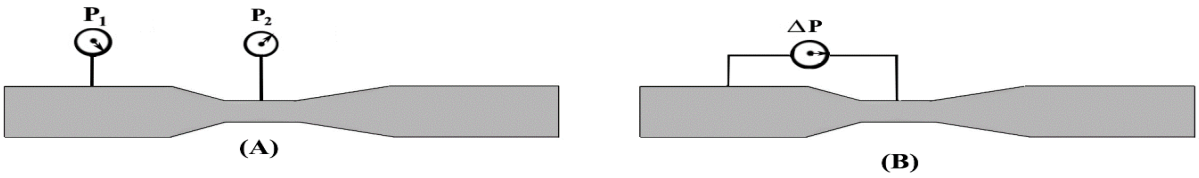

Fig. 7. different mode used for detecting type of fluid. Comparison of, A) static pressure in each part, B) static differential pressure

A. Comparison of static pressure: Table 3 to 4 show simulation results for different inlet gauge pressure of 0.4, to 1.4 and 2 bar. For instance, considering the inlet gauge pressure of 1 bar, the static pressure of air, and oxygen is 0.243 and 0.245 bar in the throat, respectively. They have 0.538 and 0.54 bar higher pressure than water with the pressure of -0.295 bar. It should be noted that the difference between the static pressure of water and other gases increases by increasing inlet gauge pressure. For example, it reaches to 1.722 bar for oxygen at input pressure of 2 bar.

Table 3. Pressure at different points for water at different inlet gauge pressure (bar)

Water	0.4	0.6	0.8	1	1.2	1.4	2
P_{t_1}	0.399	0.598	0.798	0.998	1.197	1.905	2.869
P_{t_2}	0.183	0.282	0.384	0.487	0.5919	0.696	0.955
P_{s_1}	0.398	0.597	0.797	0.996	1.195	1.3946	1.992
P_{s_2}	-0.052	-0.119	-0.201	-0.295	-0.398	-0.511	-0.877

Table 4. Pressure at different points for air at different inlet gauge pressure (bar)

Air	0.4	0.6	0.8	1	1.2	1.4	2
P_{t_1}	0.399	0.599	0.793	0.992	1.199	1.391	1.999
P_{t_2}	0.230	0.387	0.562	0.739	0.914	1.089	1.615
P_{s_1}	0.399	0.598	0.798	0.998	1.198	1.398	1.998
P_{s_2}	-0.402	0.105	0.124	0.243	0.364	0.484	0.848

Table 5. Pressure at different points for oxygen at different inlet gauge pressure (bar)

Oxygen	0.4	0.6	0.8	1	1.2	1.4	2
P_{t_1}	0.399	0.599	0.799	0.999	1.198	1.399	1.999
P_{t_2}	0.231	0.386	0.562	0.738	0.913	1.089	1.615
P_{s_1}	0.399	0.598	0.798	0.998	1.198	1.398	1.998
P_{s_2}	-0.036	0.012	0.125	0.245	0.365	0.477	0.850

B. Comparison of static differential pressure: According to Figure 8, reactant gases behave similarly. Figure 9 shows total differential pressure. It is noteworthy that the total differential pressure of water is still higher than reactant gases.

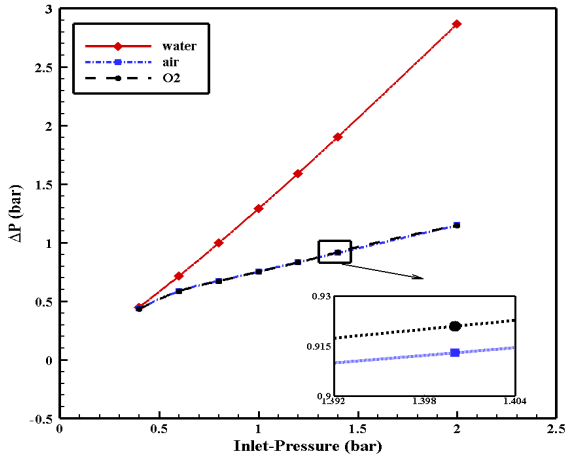

Fig.8. Differential static pressure of different fluids.

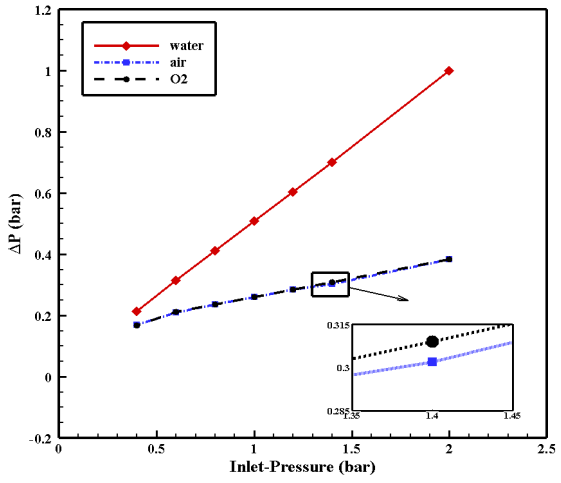

Fig. 9. Differential total pressure of different fluids.

Finally, Table 6 shows the difference between the static differential pressure of the operating gases and water. Based on the Table 6, the minimum and maximum difference is about 11.73 and 1918.13 mbar for inlet gauge pressure of 0.4 and 2 bar.

Table 6: Static Differential Pressure Differences between Reactant Gases and Water at Different Inlet Gauge Pressures

Input Pressure (bar)	$\Delta P_{Air} - \Delta P_{Water}$ (mbar)	$\Delta P_{O2} - \Delta P_{Water}$ (mbar)
0.4	11.736	15.11
0.6	129.24	130.800
0.8	323.90	325.39
1	536.64	538.06
1.2	759.36	760.58
1.4	992.08	984.46
2	1916.22	1918.13

4.2.Discharge flow rate

The discharge flow rate is one of the key points in venturi design. The diameter of the throat and convergence section should be so that not only is the discharge water greater than the produced water, but also the discharge of reactant gases should be a minimum at the time the flow type is determined. According to the diameter selected in the previous steps (0.6 mm), the flow rate for the operating fluids under different pressures is given in Table 7.

According to Table 7, the discharge flow rate of the venturi is 0.208 LPM at the inlet gauge pressure of 1 bar, which is approximately 3 times higher than the amount of water produced by the fuel cell at an electrical current intensity of 1000 A (0.0766 LPM).

Table 7. Discharge Flow Rate of Different Reactant Gases and Water

P_Inlet (bar)	Q(LPM)	Q(SLPM)	
	Water	Air	Oxygen
0.4	0.113	3.31	3.51
0.6	0.148	4.18	4.19
0.8	0.18	4.58	4.78
1	0.208	5.47	5.35
1.2	0.235	5.66	5.84
1.4	0.259	6.35	6.48
2	0.324	7.81	8.13

After detecting the type of fluid, the control system keeps the purge valve open for a few seconds. At this

time, only reactant gases pass through the venturi. As it is depicted, the flow rate for air and oxygen is 5.47 and 5.35 SLPM, respectively, for inlet gauge pressure of 1 bar. For instance, at this pressure, the fuel cell air production is 1830 SLPM, while the discharge flow rate from the venturi is 47.5 SLPM, which indicates minimal air loss.

Now, using the discharged flow rate of fluids from the fuel cell and venturi and the static pressure in the venturi (obtained from the two previous sections), the performance of the water level control system is expressed as follows. The performance of the water level control system after the separator tank is empty is describes as follows.

4.3.Control system process

A control valve is placed after the venturi to control the exiting of fluids, which is linked to the pressure sensor by the control system. There may be some water in the separator tank before the fuel cell starts to work. Therefore, the purge valve would be open in the initial state to discharge exit water from the separator tank (1). By opening the valve, the fluid enters the venturi, and the differential pressure between the convergence parts and the throat will be measured with the use of the pressure sensor (2). As explained in the previous section, the static pressure difference measured by the venturi for water is greater than reactant gases, so as long as the pressure sensor exhibits a differential pressure greater than ΔP_{s_water}, the purge valve remains open and water discharges from the separator tank (3). However, if the differential pressure became smaller than ΔP_{s_water}, one of the following models occurs:

- A sudden change in pressure due to environmental factors and the effect of the fluid flow through venturi, such as the passing of air bubbles in the water.
- Changing the type of fluid from liquid to gas.

Therefore, a period is considered to ensure the change of fluid type (4), which is displayed by $\Delta t_{critical}$. If the time of the differential pressure change stays less than $\Delta t_{critical}$, the first state occurs and the purge valve remains open, and the sensor continues measuring the static differential pressure (2). In contrast, if this time became more than $\Delta t_{critical}$, the valve would be closed (5). In the next step, depending on whether the fuel cell is turned off or not (6), the fluid separation operation ends, or the stopwatch resets for the next cycle (7). The stopwatch starts to record the time (8) and the produced water discharges to the separator tank, which has about a 60 cc capacity. The purge valve remains closed until the time indicated by the stopwatch is less than Δt_{off} (9). Then, the purge valve opens (1), and the described procedures repeat.

Figure 10 shows a flowchart of the water level control system function. The variables used in the flowchart are as follows:

$\Delta t_{critical}$: This variable is a parameter to ensure that the type of fluid has changed. The fluid passed is gas in two states. The first state is when the water in the separator tank is completely discharged, and as a result, the reactant gases begin to pass through the venturi. The second state occurs in the next cycle, right when the control system opens the purge valve after the separator tank is filled. In the first case, by closing the purge valve, the reactant gas remains inside the venturi, and the duct is attached to the separator tank. Therefore, after the valve opens, the gas leaves the system first and then the water. Because these two states happen after each other, only the suitable Δt, which supports both cases, is defined:

$$\Delta t_{critical} = C \frac{V_{net}}{A v} \tag{1}$$

In Eq.1, C,V_{net},A and V are the safety factor, control system volume, cross-section of venturi, and velocity, which are considered 1.5, 4615mm^3, 7.3 mm^2, and $\vec{V}_{Water}$ respectively. Figure11 indicates the critical time based on different inlet gauge pressures. As can be seen, the critical time decreases with the increase of inlet gauge pressure.

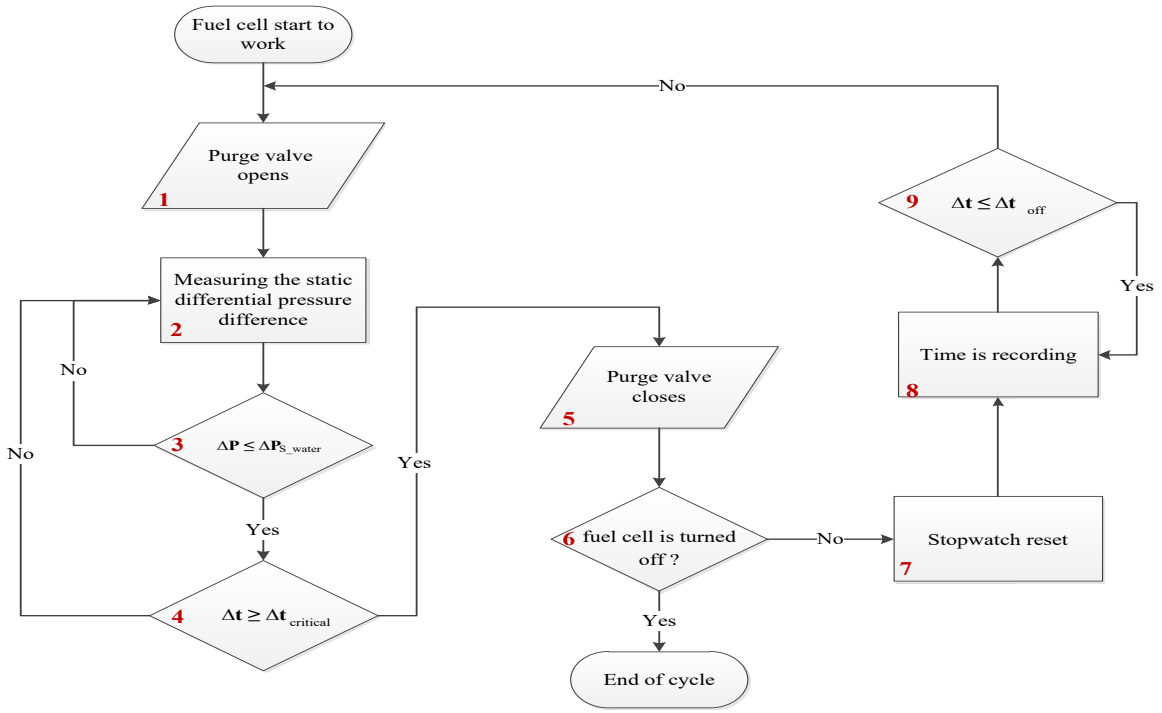

Fig.10. Function of the water level control system.

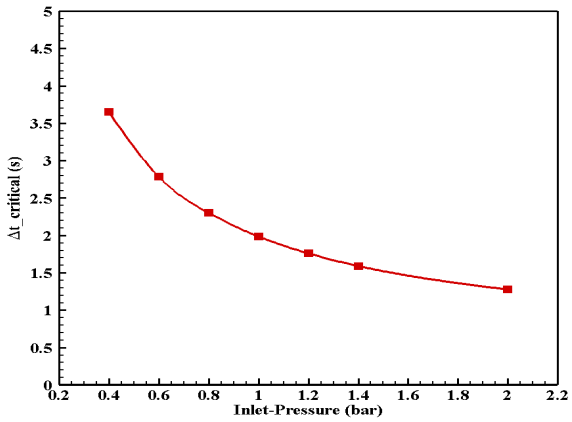

Fig.11. Critical times based on different inlet gauge pressures.

The reactant gases wasted volume is calculated by critical time and is shown in Figure 12. It is clear that by increasing the pressure of the system, the wasted volume will be reduced and experience little change for the inlet gauge pressure of more than 1.2 bar.

Δt_{off} :This parameter is defined as the time required to fill the separator tank (60 cc) based on different electrical currents and is calculated from entered water (Q_{in}) and safety factor (C). For this variable, the safety factor is considered as 1.5 in order to ensure that the level of water does not exceed the standard level in the separator tank.

$$\Delta t_{off} = \frac{1}{C}\frac{60cc}{Q_{in}} \quad (2)$$

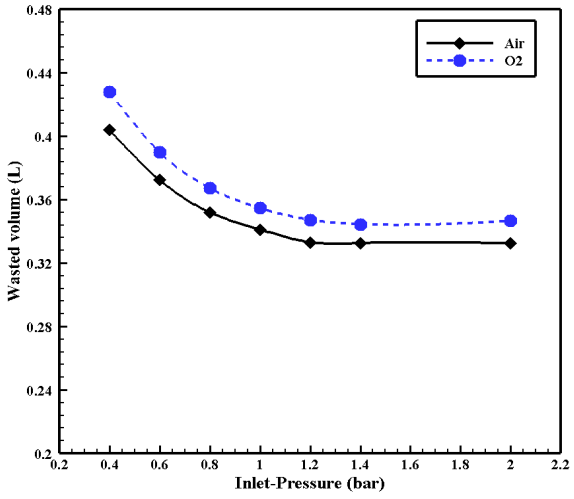

Fig.12. Discharged flow rate of reactant gases based on different inlet gauge pressures.

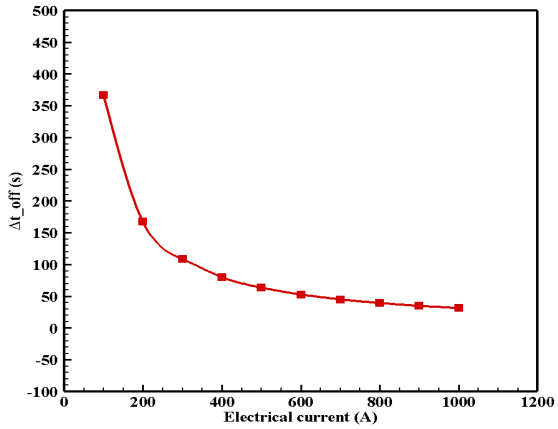

Fig.13. The time it takes to fill the separator reservoir at different electrical currents.

In other words, this parameter expresses the time the purge valve should be closed. As shown in Figure 13, this time decreases as the electrical current increases. It is worth noting that there is a dramatic decrease as the electrical current production increases from 100 to 400 A.

5.Conclusions

In this paper, an external separator control system capable of preventing the loss of reactant gases, such as oxygen, by improving the separation of water from these gases is introduced.

The separator system consists of mechanical (venturi) and control units. First, the mechanical unit, consisting of a venturi and a differential pressure sensor, measures the variations in the pressure of the fluid passing through the venturi. Then, the control unit determines the type of fluid by analyzing the data received from the mechanical unit and exports the succeeding commands to other units. Other factors investigated include:

(1) The amount of produced water and exit air was calculated based on theoretical correlation.

(2) Since the discharge flow rate is one of the key points in venturi design, two different convergence section diameters, 0.6 and 0.8, were examined. The discharge rate of the venturi with 0.6 and 0.8 mm throat diameters was 0.208 and 0.424 LPM, respectively, at the inlet gauge pressure of one bar, and the maximum discharged water for an electrical current of 1000 A was 0.0767 LPM. Although both diameters can be used, the fluid loss is lower in the case of a throat diameter of 0.6. So, this diameter was selected.

(3) There are two ways to detect the type of fluid passing through the venturi. One, the static differential pressure due to a larger pressure drop of water than reactant gases. Two, detecting the higher pressure in the throat section for gases compared to liquid.

(4) The density of oxygen is a little smaller than air, and as a result, the discharge flow rate of oxygen is more than air.

(5) The pressure drop of the fuel cell and maximum wasted volume of gases due to the use of this system is less than 0.001 bar and 0.5% in each cycle, respectively.

References

[1] Ismaier, N., J. Lersch, and A. Mattejat, Fuel cell block including a water separator. U.S. Patent No. US7,338,728 2008.

[2] Ding, Y., X. Bi, and D.P. Wilkinson, 3D simulations of the impact of two-phase flow on PEM fuel cell performance. Chemical Engineering Science, 2013. 100: p. 445-455.

[3] Adroher, X.C. and Y. Wang, Ex situ and modeling study of two-phase flow in a single channel of polymer electrolyte membrane fuel cells. Journal of Power Sources, 2011. 196(22): p. 9544-9551.

[4] Anderson, R., L. Zhang, Y. Ding, M. Blanco, X. Bi, and D.P. Wilkinson, A critical review of two-phase flow in gas flow channels of proton exchange membrane fuel cells. Journal of Power Sources, 2010. 195(15): p. 4531-4553.

[5] Rezazadeh, S. and N. Ahmadi, Numerical investigation of gas channel shape effect on proton exchange membrane

fuel cell performance. Journal of the Brazilian Society of Mechanical Sciences and Engineering, 2015. 37(3): p. 789-802.

[6] Stewart, M. and K. Arnold, Gas-liquid and Liquid-liquid Separators. 2008: Gulf Professional Publishing.

[7] Vasquez, A., K.L. McCurdy, and K.F. Bradley, Water outlet control mechanism for fuel cell system operation in variable gravity environments, U.S. Patent No. US7250075, 2007.

[8] Vasquez, A., D. Varanauski, and R. Clark Jr, Analysis and Test of a Proton Exchange Membrane Fuel Cell Power System for Space Power Applications. 2000.

[9] Charlat, P., Gas/liquid phase separator and the fuel cell-based power production unit equipped with one such separator, E.P. Patent No. EP1432493B1, 2006.

[10] Bette, W., D. Coerlin, and W. Stuhler, Fuel Cell System and Method for Operating a Fuel Cell System, E.P. Patent No. EP1761967B1, 2008.

[11] Schaefer, R. and S. Lienkamp, Laminar bypass for cascaded stack, U.S. Patent No. US7704620B2, 2010.

[12] Abdul-Razzak, A., M. Shoukri, and J.-S. Chang, Measurement of two-phase refrigerant liquid-vapor mass flow rate. Part 1: Venturi and void fraction meters. 1995, American Society of Heating, Refrigerating and Air-Conditioning Engineers, Inc., Atlanta, GA (United States).

[13] Steven, R.N., Wet gas metering with a horizontally mounted Venturi meter. Flow measurement and Instrumentation, 2002. 12(5-6): p. 361-372.

[14] Jain, T., J. Carpenter, and V.K. Saharan, CFD analysis and optimization of circular and slit venturi for cavitational activity. J. Mater. Sci. Mech. Eng, 2014. 1: p. 28-33.

[15] Meng, Z., Z. Huang, B. Wang, H. Ji, H. Li, and Y. Yan, Air–water two-phase flow measurement using a Venturi meter and an electrical resistance tomography sensor. Flow Measurement and Instrumentation, 2010. 21(3): p. 268-276.

[16] Huang, Z., D. Xie, H. Zhang, and H. Li, Gas–oil two-phase flow measurement using an electrical capacitance tomography system and a Venturi meter. Flow measurement and Instrumentation, 2005. 16(2-3): p. 177-182.

[17] Umayahara, K., S. Miura, M. Mizuno, Y. Jufuku, and M. Hasegawa, Fuel cell system and control method of same. U.S. Patent No. US7608354B2 2009.

[18] Alizadeh, E., M. Khorshidian, S. Saadat, S. Rahgoshay, and M. Rahimi-Esbo, The experimental analysis of a dead-end H2/O2 PEM fuel cell stack with cascade type design. International Journal of Hydrogen Energy, 2017. 42(16): p. 11662-11672.

[19] Illner, D., I. Mehltretter, and O. Voitlein, Method for monitoring the discharge of media out of fuel cell, and a fuel cell system, U.S. Patent No. US7413823B2 2008.
20.Barbir, F., PEM fuel cells, in Fuel Cell Technology. 2006, Springer. p. 27-51.

[21] Reader-Harris, M., Venturi Tube Design, in Orifice Plates and Venturi Tubes. 2015, Springer. p. 77-96.